Gamow-Teller strength distributions in fp-shell nuclei

P. B. Radha,[1,*] D. J. Dean,[2] S. E. Koonin,[1] K. Langanke,[3] and P. Vogel[4]
[1]*W. K. Kellogg Radiation Laboratory, California Institute of Technology, Pasadena, California 91125*
[2]*Physics Division, Oak Ridge National Laboratory, P.O. Box 2008, Oak Ridge, Tennessee 37381*
[3]*Institut for Physics and Astronomy, University of Aarhus, DK-8000 Aarhus C, Denmark*
[4]*Division of Physics, Mathematics and Astronomy, California Institute of Technology, Pasadena, California 91125*
(Received 29 July 1997)

We use the shell model Monte Carlo method to calculate complete $0f1p$-shell response functions for Gamow-Teller (GT) operators and obtain the corresponding strength distributions using a maximum entropy technique. The approach is validated against direct diagonalization for ^{48}Ti. Calculated GT strength distributions agree well with data from (n,p) and (p,n) reactions for nuclei with $A=48-64$. We also calculate the temperature evolution of the GT_+ distributions for representative nuclei and find that the GT_+ distributions broaden and the centroids shift to lower energies with increasing temperature. [S0556-2813(97)02212-7]

PACS number(s): 21.60.Cs, 21.60.Ka, 27.40.+z, 23.40.−s

I. INTRODUCTION

The Gamow-Teller (GT) properties of nuclei in the medium mass region of the periodic table are crucial determinants of the precollapse evolution of a supernova [1]. The core of a massive star at the end of hydrostatic burning is stabilized by electron degeneracy pressure as long as its mass does not exceed the appropriate Chandrasekhar mass M_{CH}. If the core mass exceeds M_{CH}, electrons are captured by nuclei. For many of the nuclei that determine the electron capture rate in this early stage of the presupernova [2], Gamow-Teller (GT) transitions contribute significantly. Due to insufficient experimental information, the GT_+ transition rates have so far been treated only qualitatively in collapse simulations, assuming the GT_+ strength to reside in a single resonance whose energy relative to the daughter ground state has been parametrized phenomenologically [3]; the total GT_+ strength has been taken from the single-particle model. However, recent (n,p) experiments [4–8], show that the GT_+ strength is fragmented over many states, and that the total strength is significantly quenched compared to the single-particle model. (A recent update of the GT_+ rates for use in supernova simulations assumed a constant quenching factor of 2 [2].)

In this paper, we describe our calculations of Gamow-Teller strength distributions in iron region nuclei: the shell model Monte Carlo (SMMC) technique is used to obtain the response functions of the Gamow-Teller operators in the full $0\hbar\omega$ fp-shell model space. These response functions are related to the strength distributions through an inverse Laplace transformation, which we carry out using a maximum entropy method.

Our starting point is the interacting shell model [9], which gives an accurate and consistent description of the properties of light nuclei [10,11] when an appropriate interaction is used. In the shell model, nucleons occupy a spectrum of single-particle orbitals that are formed by the presence of an assumed mean field. These nucleons interact through a residual effective interaction, which is derived from a realistic nucleon-nucleon potential through the G-matrix formalism [12]. The resultant interaction matrix elements require some minimal tuning to optimally account for known spectroscopic properties. In the conventional approach, the solution to the shell model is obtained by diagonalizing the nuclear Hamiltonian in a suitably chosen basis of many-particle configurations. Since the Hamiltonian matrix to be diagonalized grows combinatorially with the size of the single-particle basis and the number of valence nucleons, realistic calculations are feasible in the full fp-shell only for nuclei with $A\leqslant 50$. Hence, the traditional calculation of various nuclear properties for medium-heavy and heavy nuclei lies beyond the scope of direct-diagonalization methods except in a severely truncated model space.

The SMMC method [13–16] scales more gently with the problem size than do traditional direct-diagonalization techniques, allowing larger, and hence more realistic, calculations. This method exploits the fact that most of the billions of configurations in nuclei are unimportant for general nuclear properties, so that only a subset of the relevant configurations needs to be sampled. Observables are calculated as thermal averages in a canonical ensemble of nuclear configurations, so that nuclei at finite temperature can be studied quite naturally.

SMMC methods were used in the first complete $0\hbar\omega$ calculations for a number of ground-state [17–19], and finite-temperature properties [20] of mid-fp shell nuclei. These studies used both the Richter-Brown [21] and the KB3 [22] residual interactions. For the purposes of investigating Gamow-Teller transitions, the KB3 interaction (obtained by minimally modifying the monopole strength in the original Kuo-Brown matrix elements [24]) is well suited for full $0\hbar\omega$ studies throughout the lower-fp shell region [23]. Observables that have been calculated with this interaction in the SMMC approach include the energy $\langle H\rangle$, the total $B(E2)$, $B(M1)$, GT strengths, and various pairing properties; the calculated ground-state properties compare very well with experiment. Importantly, these studies showed that the experimentally observed quenching of the total GT strength is

*Present address: Laboratory for Laser Energetics, University of Rochester, 250 E. River Road, Rochester, NY 14623.

consistently reproduced by the correlations within the full fp shell if a renormalization of the spin operator by the factor 0.8 is invoked [19,23]. The same renormalization factor had already been deduced from sd-shell [11] and fp-shell nuclei with $A \leq 49$ [25,26] and thus appears to be universal.

In Sec. II, we reveiw the SMMC method and its application to response functions. We apply a maximum entropy (ME) method to perform the required inverse Laplace transform of the SMMC response functions; our implementation of ME for SMMC is discussed in Sec. III. Section IV includes a validation of these methods against direct diagonalization for GT transitions in ^{48}Ti, and we present GT strength functions for several heavier nuclei in the fp-shell ($A=48-64$) where experimental data are available. We also discuss the evolution of these distributions with temperature. A brief conclusion follows in Sec. V.

II. THE SHELL MODEL MONTE CARLO METHOD

The SMMC method is based on a statistical formulation of the nuclear many-body problem. In the finite-temperature version of this approach, an observable is calculated as the canonical expectation value of a corresponding operator $\hat{\mathcal{A}}$ at a given temperature T and is given by [13–16]

$$\langle \hat{\mathcal{A}} \rangle = \frac{\mathrm{Tr}_A[\hat{\mathcal{A}} e^{-\beta \hat{H}}]}{\mathrm{Tr}_A[e^{-\beta \hat{H}}]}, \tag{1}$$

where $\hat{U}=\exp(-\beta \hat{H})$ is the imaginary-time many-body propagator, $\mathrm{Tr}_A \hat{U}$ is the canonical partition function for A nucleons, $\hat{H}$ is the shell model Hamiltonian, and $\beta = 1/T$ is the inverse temperature.

In terms of a spectral expansion, the total strength of a transition operator $\hat{\mathcal{A}}$ is then given by the following expectation value:

$$B(\mathcal{A}) \equiv \langle \hat{\mathcal{A}}^\dagger \hat{\mathcal{A}} \rangle = \frac{\Sigma_{i,f} e^{-\beta E_i} |\langle f|\hat{\mathcal{A}}|i\rangle|^2}{\Sigma_i e^{-\beta E_i}}, \tag{2}$$

where $|i\rangle$ ($|f\rangle$) are the many-body states of the initial (final) nucleus with energy E_i (E_f). The total strength from the ground state can be obtained by choosing a sufficiently large value for β such that only the ground state contributes due to the Boltzmann weight.

In addition to the ''static'' strength [Eq. (2)], one can calculate for an imaginary-time τ, the response function, $R_{\mathcal{A}}(\tau)$, which describes dynamical behavior and contains information about the nuclear spectrum:

$$R_{\mathcal{A}}(\tau) \equiv \langle \hat{\mathcal{A}}^\dagger(\tau) \hat{\mathcal{A}}(0) \rangle = \frac{\mathrm{Tr}_A[e^{-(\beta-\tau)\hat{H}} \hat{\mathcal{A}}^\dagger e^{-\tau \hat{H}} \hat{\mathcal{A}}]}{\mathrm{Tr}_A[e^{-\beta \hat{H}}]}$$

$$= \frac{\Sigma_{if} e^{-\beta E_i} e^{-\tau(E_f - E_i)} |\langle f|\hat{\mathcal{A}}|i\rangle|^2}{\Sigma_i e^{-\beta E_i}}. \tag{3}$$

The strength distribution

$$S_{\mathcal{A}}(E) = \frac{\Sigma_{if} \delta(E - E_f + E_i) e^{-\beta E_i} |\langle f|\hat{\mathcal{A}}|i\rangle|^2}{\Sigma_i e^{-\beta E_i}} \tag{4}$$

is related to $R_{\mathcal{A}}(\tau)$ by a Laplace transform:

$$R_{\mathcal{A}}(\tau) = \int_{-\infty}^{\infty} S_{\mathcal{A}}(E) e^{-\tau E} dE. \tag{5}$$

Note from Eq. (3) that ground-state to ground-state transitions require large $(\beta - \tau)$ in addition to large β. The large-τ behavior of $R_{\mathcal{A}}$ allows, in principle, a measurement of the specific transition between the ground state and the lowest allowed final state by the operator; the slope of $\log_e [R(\tau)]$ in this limit provides the transition energy, and the intercept measures the transition strength.

The SMMC canonical expectation values are based on the discretization of the many-body propagator $e^{-\beta H}$ into a finite number of ''time'' slices N_t each of duration $\Delta\beta = \beta/N_t$. At each time slice the many-body propagator is linearized via the Hubbard-Stratonovich transformation [27,28]; observables are thus expressed as path integrals of one-body propagators in fluctuating auxiliary fields. The integration is carried out by a Metropolis random walk [29].

To circumvent the ''sign problem'' encountered in the SMMC calculations with realistic interactions, we use the extrapolation procedure outlined in Refs. [17,20]. Yet another, but distinct, source of the sign problem is an odd number of nucleons in the canonical expectation values [16]. We overcome this problem by a number-projection technique, first employed in [18] and subsequently used in [16], that allows us to extract information concerning odd-A nuclei from the neighboring even-even system.

III. THE METHOD OF MAXIMUM ENTROPY

Once we have the Gamow-Teller response functions, they must be inverted to obtain strength distributions. The inverse of the Laplace transform (5) required to extract the strength functions is an ill-conditioned numerical problem [30]. The kernel (which in this case is $e^{-\tau E}$) acts as a smoothing operator and thus the solution, for which the kernel must be inverted, will be extremely sensitive to small changes (i.e., to errors) in the input data. In this section, we describe a maximum entropy procedure to carry out the inversion [16].

Consider the χ^2 deviation of the data, $r_i \equiv R(\tau = i\Delta\beta)$, with errors σ_i from the fit values $F_i\{S\}$ produced by the trial inverse and obtained according to Eq. (5):

$$\chi^2\{S\} = \sum_i \left(\frac{r_i - F_i\{S\}}{\sigma_i} \right)^2. \tag{6}$$

Direct minimization of χ^2 is numerically stable only in the simplest of circumstances (such as few-parameter data fitting). Combining χ^2 with some other auxiliary well-conditioned functional $P\{S\}$ such that $P\{S\}$ has a minimum at the smooth solution $S(E)$ and penalizes strongly oscillating functions, leads to a compromise between fitting the data and the expected smoothness of the inverse. Thus one minimizes the joint functional

$$\frac{1}{2}\chi^2\{S\} + P\{S\}. \tag{7}$$

The functional $P\{S\}$ is chosen as the information theoretic entropy,

$$P\{S\}=\alpha\int dE\left[m(E)-S(E)+S(E)\ln\left(\frac{S(E)}{m(E)}\right)\right], \quad (8)$$

where $m(E)$ is a default model and α is an adjustable parameter that both specify the *a priori* knowledge of $S(E)$.

In order to minimize the functional (7), we employ the technique of Ref. [31], which involves an iterative sequence of linear programming problems. We first expand Eq. (8) to second order in $S(E)$ about some positive function $f(E)$ to obtain

$$P\{f|S\}=\alpha\int dE\left\{\left(m-\frac{f}{2}\right)+\left[\ln\left(\frac{f}{m}\right)-1\right]S+\frac{S^2}{2f}\right\}. \quad (9)$$

If the true minimum $S(E)$ of the nonquadratic functional in Eq. (8) is taken as a point of expansion of $f(E)$ in [Eq. (9)], then it also gives the minimum of the corresponding quadratic functional

$$S(E)=\min_a\left[\frac{1}{2}\chi^2\{a\}+P\{S|a\}\right]. \quad (10)$$

Since we require extraction of positive strength function, we iterate while retaining partially the result of the previous iteration as

$$S^{(n+1)}=\min_{S\geqslant 0}\left[\frac{1}{2}\chi^2\{S\}+P\{f^{(n)}|S\}\right], \quad (11)$$

with

$$f^{(n)}(E)=\xi S^{(n-1)}(E)+(1-\xi)S^{(n)}(E), \quad (12)$$

and the default model as the starting approximation to S,

$$S^{(0)}(E)=S^{(-1)}(E)\equiv m(E). \quad (13)$$

The rate of convergence and stability are controlled by the mixing parameter $0<\xi<1$; a value of $\xi=0.3$ is a reasonable choice to guarantee stability. Typically, convergence to the ''true'' solution is obtained in less than 40 iterations. In this way, the minimization of a general functional that is intrinsic to a maximum entropy approach is reduced to an iterative procedure in which each step requires the minimization of a quadratic functional with linear inequality constraints.

Some general remarks regarding this inversion technique are called for. Since $R(\tau)$ is calculated at discrete values of imaginary time and, in principle, up to an imaginary time β, the smallest energy that can be resolved in $S(E)$ is of order $1/\beta$, and the largest is the inverse of the discretization size $1/\Delta\beta$. In practice, numerical noise forces a cutoff in the largest τ value that can be used, thus decreasing the energy resolution.

As we mentioned above, the default model can be chosen by investigating the characteristics of the response function. From Eq. (3), one sees that $d\ln[R(\tau)]/d\tau|_{\tau=0}$ gives the centroid of the distribution in the parent nucleus, and thus in the case of the GT_+ operator we choose for the default model a Gaussian with a peak at this energy and with a width of 1.5−2 MeV; this width can be estimated from $d^2\ln[R(\tau)]/d\tau^2|_{\tau=0}$. The parameter α is the inverse of the total strength of the distribution, and is calculated from the default model as $\alpha=[\int dE\,m(E)]^{-1}$. In the case of the GT_- operator, we make a better guess for the default model by including some features of the distribution. Experimental distributions typically have three regions: the $T=T_z$ and $T=T_z+1$ regions distributed around 6 and 12 MeV, respectively, and a more fragmented region at lower energies. We choose for our GT_- default model two Gaussians with the same widths, each centered at the appropriate energy. The lower energy part of the distributions is governed by the high τ region of the response function. Although this region of the response function is sometimes contaminated by large statistical fluctuations, the reconstruction tends to give a low-energy peak that well describes these more discrete transitions.

IV. GAMOW-TELLER STRENGTH DISTRIBUTIONS

The GT operators are defined as $\mathbf{GT}_\pm=\Sigma_l\boldsymbol{\sigma}_l\tau_l^\pm$, where $\boldsymbol{\sigma}_l$ is the Pauli spin operator for nucleon l and τ_l^- (τ_l^+) is the isospin lowering (raising) operator that changes a neutron (proton) into a proton (neutron); they thus describe charge-changing decay modes. GT strength distributions play an important role in two very different contexts. In the astrophysical context, medium-heavy nuclei at a finite temperature in the core of a presupernova capture electrons. A strong phase space dependence makes the relevant electron capture rates more sensitive to GT *distributions* than to total strengths [32,33] and thus necessitates complete $0\hbar\omega$ calculations of these distributions. GT strengths are also important in studies of double β decay [34]. The two-neutrino mode of this decay, which provides important confidence in extracting the neutrino mass from zero-neutrino decay experiments, is equivalent to a description of the GT strength functions from the ground states of the parent and daughter nuclei. Thus, any reliable calculation of the two-neutrino matrix element must accurately describe these strength distributions.

In the following sections we demonstrate and validate the ME method for the GT operator by comparing our results with direct diagonalization. We then compare our results with experimentally obtained distributions for various fp-shell nuclei. In what follows we will use the renormalized GT operator corresponding to $\mathbf{GT}_\pm/1.26$ [19,23].

A. Comparison with direct diagonalization

Direct-diagonalization results in the complete fp shell can be obtained for nuclei with $A\leqslant 48$. We choose ^{48}Ti for a comparison and in Fig. 1, we show our results for this nucleus. The lower left-most panel shows the GT_+ response function $R(\tau)$ for ^{48}Ti as measured in the parent and the middle lower panel shows the extracted strength distribution $S(E)$ in the daughter ^{48}Sc. Also shown in the same panel is the direct-diagonalization result [35]. The discrete transitions found in the direct diagonalization have been smeared with a Gaussian of width 0.25 MeV in order to facilitate comparisons. While the SMMC total strength (i.e., the area under the curve) $B(GT_+)=0.72\pm0.11$ [19] compares very well with the direct-diagonalization value of 0.79 [23], the SMMC can recover only gross features of this distribution. In particular,

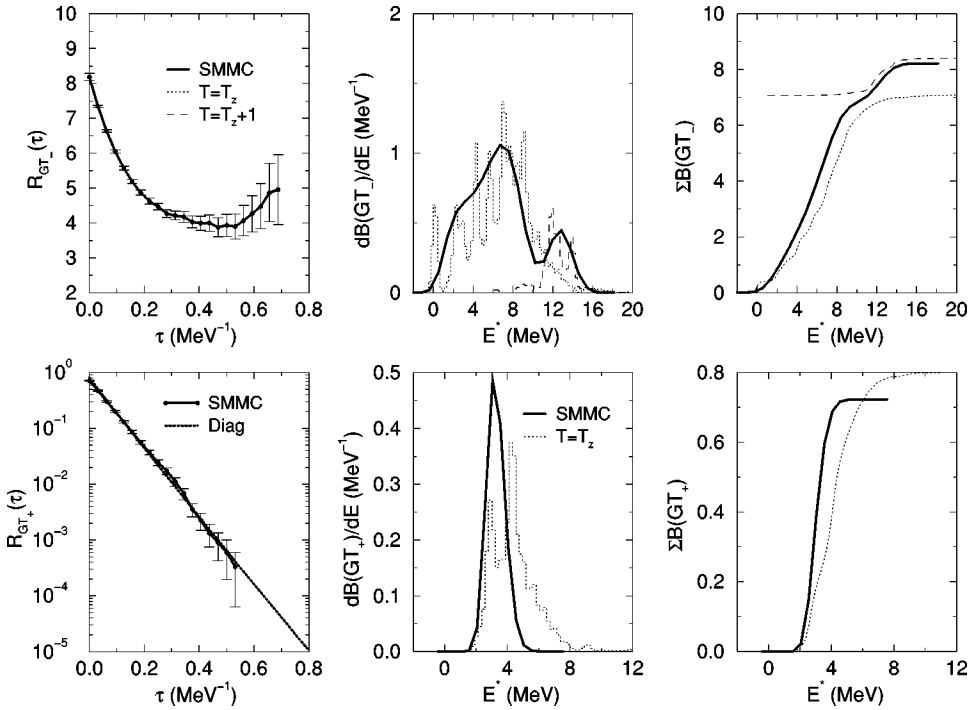

FIG. 1. Left-most panels show the GT_- (upper) and GT_+ (lower) response functions calculated through the SMMC. The middle panels show the corresponding strength function and direct-diagonalization results [23,35] in the corresponding daughter. For the GT_- we show both the $T=T_z$ and $T=T_z+1$ channels, while the dash-dot line in the GT_+ distribution comes from folding the SMMC results with a Gaussian corresponding to the experimental sensitivity. The right-most panels show the cumulative strengths as a function of the daughter excitation energy. For the GT_- we show the cumulative $T=T_z+1$ strength starting from the total in the $T=T_z$ channel.

the peak is somewhat too narrow, mainly due to the information lost by the Laplace transform. This attribution was checked by calculating the response function $R(\tau)$ for the direct diagonalization distribution. (The peaks were smeared by Gaussians of 0.25 MeV width to account for the SMMC finite discretization.) This response function is shown in the lower left panel of Fig. 1, and agrees well with the SMMC result.

The lower right-most panel in Fig. 1 shows the energy dependence of the cumulative strength $\int_0^{E^\star} S(E')dE'$, where $E^\star$ is the excitation energy in the daughter. One can see that the SMMC recovers the centroid and the width of the distribution reasonably.

A brief remark about the possible sources of error is in order. Since our ME procedure provides a most probable extraction of the strength function, the strength distributions do not have error bars associated with them. However, from the SMMC error bars for $R(\tau)$, we estimate the error in the position of the centroid to be about 0.5 MeV. In addition, we note that the response functions are measured in the parent nucleus, and to obtain the energy in the daughter we use the experimental mass excesses and a parametrization of the Coulomb energy as defined in [23]. [In the test case (^{48}Ti), we exactly calculate this mass difference.] This parametrization provides a good overall description of the masses of the nuclei in this region [19]. We find an average deviation between 0.1 MeV (for $A=48$ nuclei) and 0.5 MeV (for $A=54$ nuclei) of our calculated binding energies from experimental values, suggesting that our procedure is quite justified.

The upper panels of Fig. 1 show our results for the GT_- operator in ^{48}Ti. The total strength $B(GT_-)$ can be readily obtained from the renormalized Ikeda sum rule $B(GT_-)-B(GT_+)=3(N-Z)/(1.26)^2$ which is obeyed by both the SMMC and direct-diagonalization calculations. The GT_- operator takes the $N>Z$ parent nucleus (with $T=T_z+1$) to $T=T_z$(dotted), $T=T_z+1$ (dashed), and $T=T_z+2$ (not shown) states in the ^{48}V daughter. The $T=T_z$ states are the lowest in energy and contain most (85% in this case) of the strength. Assuming in the default model that the centroid of the $T=T_z+1$ states is located 5 MeV higher than the centroid of the $T=T_z$ states, we obtain a good reproduction of both components of the strength distribution. This general assumption is experimentally valid in the even-even nuclei in this region. We also see at low energy a hint of the discrete low-energy states in the reconstruction.

B. Comparison with experiment

Experimental GT distributions are obtained from intermediate-energy charge exchange (n,p) [or (p,n)] cross sections at forward angles, which are proportional to the GT strength [38]. These experimental distributions typically extend only to 8 MeV in the daughter nucleus to exclude contributions from other multipolarities.

We first compare our ^{48}Ti result for the GT_+ distribution against experiment, as shown in Fig. 2. To simulate the finite experimental resolution and presentation of the data, the SMMC results have been smeared with Gaussians of standard deviation of 1.77 MeV, following Ref. [39]. Our results are represented by the dotted line in Fig. 2, while the diagonalization results are shown as a solid histogram. The smeared diagonalization result is shown by the dashed line in

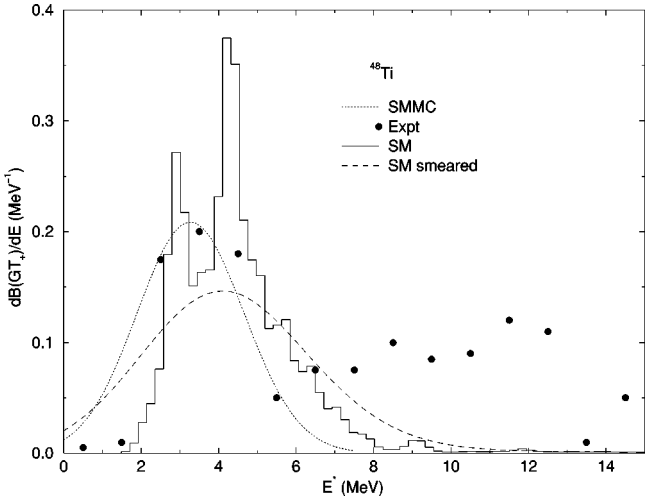

FIG. 2. Calculated strength function (smeared by the experimental resolution) for the GT_+ operator for ^{48}Ti compared to the experimental data [5]. Also shown is the shell model spectrum obtained by diagonalization, and smeared by 0.25 MeV (histogram) and by 1.77 MeV (dashed line) to account for the experimental resolution.

the figure. The experimental $B(GT_+)$ distribution, shown as solid dots, sums 1.42 ± 0.2 [5] compared to our renormalized value of 0.71 ± 0.11. We find that the calculated $0\hbar\omega$ GT_+ strength extends only over the region $E^\star<8$ MeV [in agreement with the experimental value for this range of energy $B(GT_+)=0.77\pm0.1$]. Whether the observed strength for $E^\star>8$ MeV is indeed the missing GT strength and might be related to correlations outside the $0\hbar\omega$ model space is still under debate. We refer the reader to the work in Refs. [23,36]. The quenching of the GT strength for pf shell nuclei is also discussed in [37], although the calculations presented there were performed in severely truncated shell model spaces. We note that the inadequacy of a $0\hbar\omega$ model space to describe the GT_+ distribution at $E^\star>8$ MeV might have some relevance to the $\beta\beta$ decay of ^{48}Ca [40], where considerable $2\nu\beta\beta$ strength could be obtained from the overlap of this distribution with that of ^{48}Ca in the (p,n) direction for these energies. However, the measured $2\nu\beta\beta$ decay rate of ^{48}Ca [41] agrees well with the calculation based on the $0\hbar\omega$ shell model, which includes the 1/1.26 normalization of the GT transition operator.

We now turn to a comparison of SMMC results with experiment for nuclei in the mid-fp shell where complete direct-diagonalization calculations are not possible. We first consider the (n,p) reaction and in Fig. 3 we show our results for all even-even nuclei with $A=48-64$ for which data are available [4,6,7]. The SMMC results have been smeared with Gaussians of standard deviation of 1.77 MeV to account for the finite experimental resolution, following Ref. [39]. Experimentally, the GT_+ strength is significantly fragmented over many states; the centroids and the widths of these distributions are reproduced very well in the SMMC approach. We note in Fig. 3 that the experimental GT distributions show larger strengths at energies $E^\star>6$ MeV than the calculations. This is similar to the case of ^{48}Ti discussed above and might indicate again that the reproduction of the GT strength at higher excitation energies requires the inclusion

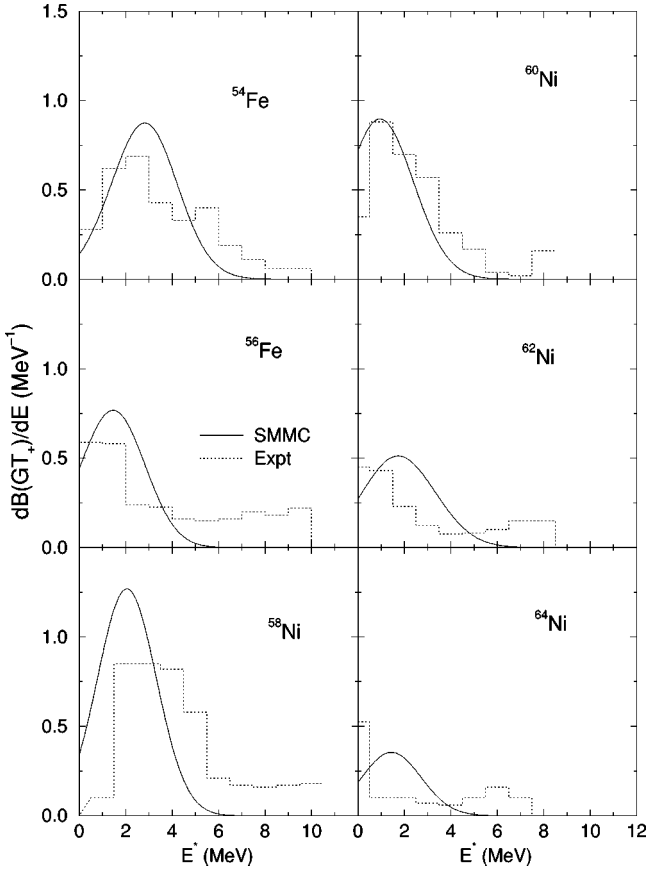

FIG. 3. Comparison of calculated GT_+ strength distribution against experiment [4,7,42,43] for even-even nuclei as function of excitation energy in the corresponding daughter nuclei.

of configurations outside the $0\hbar\omega$ model space. Our results for the total strengths are given in Table I.

SMMC results for odd-A nuclei in the (n,p) direction are shown in Fig. 4, where again the centroids and widths of the distributions are in good agreement with the data [7,42,43].

TABLE I. Renormalized $B(GT_+)$ strengths as calculated in the SMMC approach compared to experimental strengths [4,7,42,43]. The superscripts on the experimental results indicate the upper limit of energies used to obtain the total strength.

Nucleus	$B(GT_+)$ (SMMC)	$B(GT_+)$ (expt)
^{48}Ti	0.71 ± 0.11	1.31 ± 0.2 [a]
^{51}V	1.40 ± 0.14	1.48 ± 0.03 [b]
^{54}Fe	3.84 ± 0.28	$3.1\ \pm0.6$ [c]
^{55}Mn	1.84 ± 0.36	$1.7\ \pm0.2$ [d]
^{56}Fe	2.51 ± 0.17	$2.9\ \pm0.3$ [d]
^{58}Ni	4.23 ± 0.31	$3.8\ \pm0.4$ [d]
^{59}Co	2.60 ± 0.31	2.39 ± 0.07 [b]
^{60}Ni	3.26 ± 0.25	3.11 ± 0.08 [e]
^{62}Ni	2.16 ± 0.25	2.53 ± 0.07 [e]
^{64}Ni	1.09 ± 0.18	1.72 ± 0.09 [e]

[a]Up to 14 MeV.
[b]Up to 12.5 MeV.
[c]Up to 10 MeV.
[d]Up to 8.5 MeV.
[e]Up to 8 MeV.

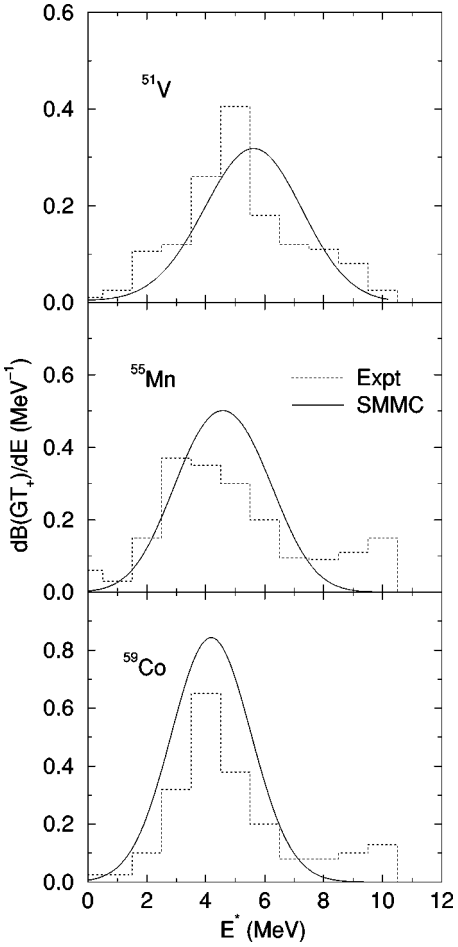

FIG. 4. Calculated GT_+ distributions for odd-A nuclei. Also shown are the experimental distributions [7,42,43]. The energies are in the corresponding daughter.

Calculations for odd-A nuclei are performed at a finite temperature of 0.8 MeV. (The temperature dependence of these distributions will be discussed later in Sec. IV C.) The response functions for the three nuclei in Fig. 4 are sampled from the partition functions of their neighbors, i.e., ^{51}V from ^{52}Cr, ^{55}Mn from ^{56}Fe, and ^{59}Co from ^{60}Ni. The peaks of the observed GT_+ distributions in odd-A nuclei in Fig. 4 are consistently at higher excitation energies in the daughter compared to the even-even cases in Fig. 3, a feature reproduced by the SMMC calculations. These higher excitation energies cause some $0\hbar\omega$ strength to lie above the typical 8 MeV cutoff in odd-A nuclei. The data for ^{51}V and ^{59}Co have been analyzed for additional strength above 8 MeV [32,33] (see Table I), while, to our knowledge, ^{55}Mn has not been reanalyzed for potential GT strength at $E^\star > 8$ MeV. For even-even nuclei the $0\hbar\omega$ GT_+ strength appears to be exhausted at energies below 8 MeV, in agreement with the SMMC results shown in Fig. 3. Our results for ^{51}V and ^{55}Mn show some strength above 8 MeV, but this is not the case for ^{59}Co.

In Fig. 5 we compare the GT_- distributions for a few nuclei where experimental data are available [6,44]; the experimental data for ^{56}Fe have been obtained from Ref. [39]. From the cumulative strengths in the right panels of Fig. 5, we can conclude that the SMMC approach reproduces the experimental distribution moderately well for the cases of

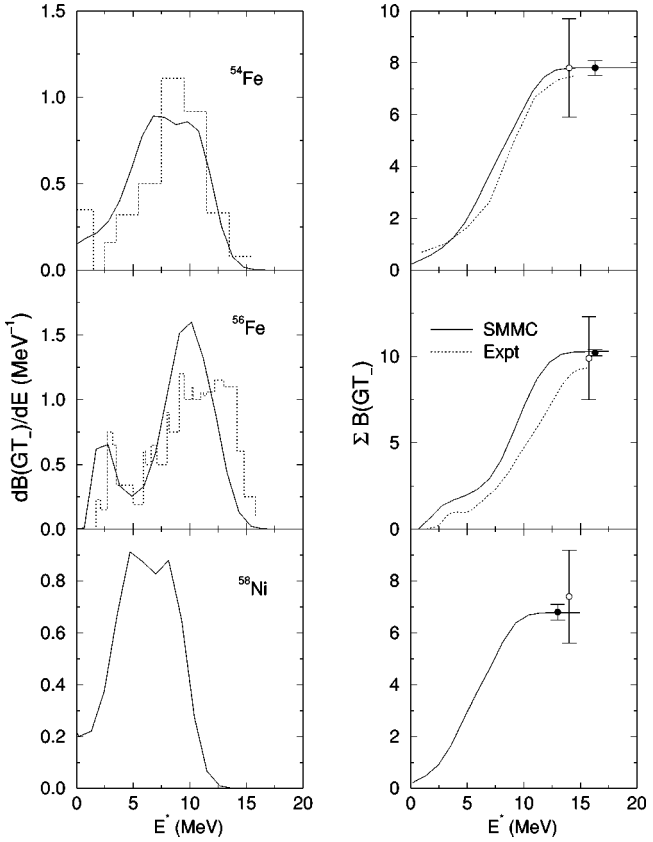

FIG. 5. Left panels: Calculated GT_- distributions for several nuclei in the mid-fp shell against distributions obtained from (p,n) reactions [6,44]. Right panels: Cumulative strength distributions versus daughter excitation energy for SMMC calculations and experiment. $B(GT_-)$ from SMMC (solid circles) and from experiment (open circles) are shown staggered for clarity.

^{54}Fe and ^{56}Fe. For the Ni isotopes, only partial information is available about these distributions. For ^{58}Ni the peaks in the experimental data [44] shown are to be associated with a finite width 1.3, 0.7, and 0.5 MeV for the peaks at 9.2, 11.2, and 13.0 MeV, respectively. The strength in the giant resonance region between 6.4 and 13.0 MeV is quoted as 5.5, while we obtain 6.1, which is consistent with the uncertainty in the excitation energy. For ^{60}Ni the experimental value of the total GT_+ strength [44] is 7.2 ± 1.8 whereas we obtain 10.87 ± 0.23. As our calculation obeys the renormalized Ikeda sum rule and reproduces the measured GT_+ strength, the lower experimental value indicates some strength outside the experimental window of $E^\star > 14$ MeV. We also note that while Ref. [44] quotes an integrated strength of 6.22 between 4.0 and 14.0 MeV we obtain a value of 4.65.

C. Temperature dependence of GT strengths

We now turn to the temperature evolution of GT_+ strength functions. Representative strength distributions for two nuclei, ^{59}Co and ^{60}Ni, at several temperatures are shown in Fig. 6. Both figures are plotted as a function of E, the energy transfer to the parent nucleus. We note that the restriction of the model space to only fp-shell renders our calculation quantitatively unreliable for even-even nuclei at $T \gtrsim 1.4$ MeV [20], while for the odd-A cases this temperature is likely even lower.

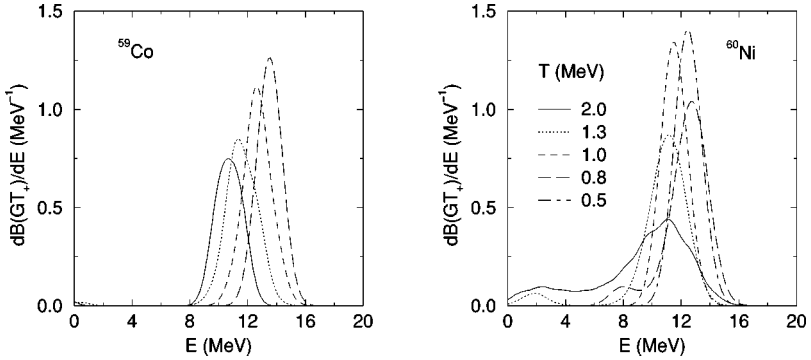

FIG. 6. Temperature evolution of GT_+ strength distribution for sample nuclei (left: ^{59}Co; right: ^{60}Ni) versus parent excitation energy.

With increasing temperature, three distinct effects occur that influence the GT strength distributions.

(i) The number of states contributing to the thermal ensemble increases. Due to the pairing gap in even-even nuclei, this occurs at a higher temperatures in even-even nuclei than in odd-A nuclei.

(ii) GT transitions which are Pauli blocked at low temperatures due to closed neutron subshells (e.g., the $f_{7/2}$ orbital) can become thermally unblocked as neutrons are moved to excited orbitals with increasing temperature. Similarly, protons which are thermally excited to higher orbitals can undergo allowed GT transitions.

(iii) The ground state in even-even nuclei is dominated by like-nucleon pairing. As indicated by SMMC calculations, these pairs break at around $T=1$ MeV. Thus at low temperatures, a GT_+ transition involves breaking a proton pair associated with an extra energy of 1–2 MeV. This ''penalty energy'' is removed at higher temperatures in states of higher excitation energy, in which the pair correlations are diminished.

As we will discuss in the following, these three effects allow for an understanding of the temperature dependence of the GT_+ strength distributions.

In the case of ^{59}Co, with increasing temperature, the entire distribution shifts to lower excitation energies. The total strength decreases and the width of the distribution increases marginally with increasing temperatures. [We have checked that in the high-T limit, $B(GT_+)$ rises to the single-particle value as expected.] Due to the lack of pairing of the odd particle in an odd-A nucleus, states of various spins are more quickly populated than in the even-even systems. These states then make transitions to daughter states by the GT operator. Thus, a plethora of states is easily accessible at moderate temperatures, and the required excitation energy in the daughter is lower.

For ^{60}Ni, the peak in the strength distribution remains roughly constant with increasing temperature, while the width increases with the appearance of low-lying strength due to transitions from the thermally occupied to the empty excited orbitals. Note also that the centroid of the distribution remains constant at the low temperatures and then shifts to lower excitation at higher temperatures. The near constancy of the peak position in ^{60}Ni at low temperatures supports the shifting assumption (attributed to Brink in Ref. [45]) which states that the centroid corresponding to each parent excited state is shifted upward in the daughter nucleus by the energy of the parent state [45]. This hypothesis assumes that the internal configuration of the low-lying states is roughly the same. With increasing temperature, however, states with other internal configurations gain statistical weight, and in particular, the pair correlations in these excited states decrease. SMMC calculations indicate that pairs break around $T=1$ MeV in even-even nuclei, allowing for a dramatic increase in thermally populated states in the parent at and above this temperature. For these excited states, no coherence energy has to be paid as penalty to break a proton pair in the GT transition, and the peak in the GT distribution moves to smaller energies. We also note that at temperatures $T\leqslant 1.3$ MeV the thermal ensemble already includes the lowest excited $T+1$ states allowing for transitions at $E=0$. In contrast, these transitions are not observed in ^{59}Co at the temperatures considered here, since the $T+1$ states in this nuclei are at higher excited energies due to the larger neutron excess. We also observe a gradual decrease of the peak position with temperature in accordance with the fact that no pairing gap has to be overcome in odd-A nuclei.

V. SUMMARY AND CONCLUSIONS

As mentioned in the Introduction, electron capture on iron region nuclei plays an important role at the onset of core collapse in a massive star. Under these conditions, nuclei have a finite temperature of $0.2-0.6$ MeV. It is well known that for nuclei with an opened fp-shell neutron configuration, GT_+ transitions dominate the electron capture rate, and a strong phase-space dependence makes the rate sensitive to the full GT_+ distribution, rather than only to the total strength. Unfortunately, the GT_+ strength is not experimentally accessible for those nuclei of importance in the presupernova collapse. Thus, collapse studies have to rely on theoretical estimates which, until recently, could not be performed with great confidence. This has now changed. As SMMC calculations reproduce the measured data from first principles without nucleus-specific data fitting (which has been necessary in previous studies), they are reliable enough to predict the GT_+ distributions for those astrophysically important nuclei not experimentally accessible. SMMC calculations for these nuclei are in progress.

In this paper, we have calculated response functions for the Gamow-Teller operators for several nuclei in the fp shell. We use the KB3 interaction, which is well suited for $0\hbar\omega$ calculations. Using an implementation of the ME technique, we have then obtained the corresponding strength distributions.

The extracted Gamow-Teller distributions compare very well with both direct-diagonalization calculations and the experimentally obtained distributions. We note that we invoke the standard renormalization factor of 1/1.26 for the transition operator, in keeping with the observation in sd- and fp-shell nuclei that complete $0\hbar\omega$ calculations require this overall renormalization for agreement with experiment.

We have also studied the effect of finite temperature on Gamow-Teller distributions and have demonstrated for sample nuclei that our calculations at $T=0.8$ MeV should be adequate to describe the distributions required to calculate electron capture rates for the presupernova problem [2]. Studies of the Gamow-Teller strengths and electron capture rates for nuclei relevant to the presupernova collapse will be described elsewhere.

ACKNOWLEDGMENTS

We acknowledge support from the U.S. National Science Foundation under Grant Nos. PHY94-12818 and PHY94-20470. Oak Ridge National Laboratory is managed by Lockheed Martin Energy Research Corp. for the U.S. Department of Energy under Contract No. DE-AC05-96OR22464. K.L. has been partly supported by the Danish Research Council. Grants of computational resources were provided by the Center for Advanced Computational Research at Caltech and the Center of Computational Science at ORNL.

[1] H. A. Bethe, Rev. Mod. Phys. **64**, 491 (1992).
[2] M. B. Aufderheide, I. Fushiki, S. E. Woosley, and D. H. Hartmann, Astrophys. J. **91**, 389 (1994).
[3] G. M. Fuller, W. A. Fowler, and M. J. Newman, Astrophys. J. **S42**, 447 (1980); **48**, 279 (1982); **252**, 715 (1982); **293**, 1 (1985).
[4] A. L. Williams *et al.*, Phys. Rev. C **51**, 1144 (1995).
[5] W. P. Alford *et al.*, Nucl. Phys. **A514**, 49 (1990).
[6] M. C. Vetterli *et al.*, Phys. Rev. C **40**, 559 (1989).
[7] S. El-Kateb *et al.*, Phys. Rev. C **49**, 3129 (1994).
[8] T. Rönnquist *et al.*, Nucl. Phys. **A563**, 225 (1993).
[9] M. Mayer and J. Jensen, *Elementary Theory of Nuclear Shell Structure* (Wiley, New York, 1955).
[10] S. Cohen and D. Kurath, Nucl. Phys. **73**, 1 (1965).
[11] B. Brown and B. Wildenthal, Annu. Rev. Nucl. Part. Sci. **38**, 29 (1988).
[12] M. Hjorth-Jensen, T. T. S. Kuo, and E. Osnes, Phys. Rep. **261**, 125 (1995), and references therein.
[13] C. W. Johnson, S. E. Koonin, G. H. Lang, and W. E. Ormand, Phys. Rev. Lett. **69**, 3157 (1992).
[14] G. H. Lang, C. W. Johnson, S. E. Koonin, and W. E. Ormand, Phys. Rev. C **48**, 1518 (1993).
[15] W. E. Ormand, D. J. Dean, C. W. Johnson, G. H. Lang, and S. E. Koonin, Phys. Rev. C **49**, 1422 (1994).
[16] S. E. Koonin, D. J. Dean, and K. Langanke, Phys. Rep. **278**, 1 (1997).
[17] Y. Alhassid, D. J. Dean, S. E. Koonin, G. Lang, and W. E. Ormand, Phys. Rev. Lett. **72**, 613 (1994).
[18] D. J. Dean, B. P. Radha, K. Langanke, S. E. Koonin, Y. Alhassid, and W. E. Ormand, Phys. Rev. Lett. **72**, 4066 (1994).
[19] K. Langanke, D. J. Dean, P. B. Radha, Y. Alhassid, and S. E. Koonin, Phys. Rev. C **52**, 718 (1995).
[20] D. J. Dean, S. E. Koonin, K. Langanke, P. B. Radha, and Y. Alhassid, Phys. Rev. Lett. **74**, 2909 (1995).
[21] W. A. Richter, M. G. Vandermerwe, R. E. Julies, and B. A. Brown, Nucl. Phys. **A523**, 325 (1991).
[22] A. Poves and A. Zuker, Phys. Rep. **70**, 235 (1981).
[23] E. Caurier, A. Zuker, A. Poves, and G. Martinez-Pinedo, Phys. Rev. C **50**, 225 (1994).
[24] T. T. S. Kuo and G. E. Brown, Nucl. Phys. **A114**, 241 (1968).
[25] G. Martinez-Pinedo, A. Poves, E. Caurier, and A. P. Zuker, Phys. Rev. C **53**, R2602 (1996).
[26] G. Martinez-Pinedo, A. P. Zuker, A. Poves, and E. Caurier, Phys. Rev. C **55**, 187 (1997).
[27] J. Hubbard, Phys. Rev. Lett. **3**, 77 (1959).
[28] R. Stratonovich, Dokl. Akad. Nauk SSSR **115**, 1097 (1957).
[29] N. Metropolis, A. Rosenbluth, M. Rosenbluth, A. Teller, and E. Teller, J. Chem. Phys. **21**, 1087 (1953).
[30] W. H. Press, S. A. Teukolsky, W. T. Vetterling, and B. P. Flannery, *Numerical Recipes in FORTRAN* (Cambridge University Press, Cambridge, England, 1992).
[31] S. Meshkov and D. Berkov, Int. J. Mod. Phys. C **5**, 987 (1994).
[32] M. B. Aufderheide, S. D. Bloom, D. A. Ressler, and G. J. Mathews, Phys. Rev. C **47**, 2961 (1993).
[33] M. B. Aufderheide, S. D. Bloom, D. A Ressler, and G. J. Mathews, Phys. Rev. C **48**, 1677 (1993).
[34] F. Boehm and P. Vogel, *Physics of Massive Neutrinos* (Cambridge University Press, New York, 1987).
[35] E. Caurier, A. Poves, and A. Zuker, Phys. Lett. B **252**, 13 (1990).
[36] E. Caurier, A. Poves, and A. P. Zuker, Phys. Rev. Lett. **74**, 1517 (1995).
[37] N. Auerbach, G. F. Bertsch, B. A. Brown, and L. Zhao, Nucl. Phys. **A556**, 190 (1993).
[38] G. F. Bertsch and H. Esbensen, Rep. Prog. Phys. **50**, 607 (1987).
[39] E. Caurier, G. Martinez-Pindeo, A. Poves, and A. P. Zuker, Phys. Rev. C **52**, R1736 (1995).
[40] A. Poves, P. B. Radha, K. Langanke, and P. Vogel, Phys. Lett. B **361**, 1 (1995).
[41] A. Balysh *et al.*, Phys. Rev. Lett. **77**, 5186 (1997).
[42] J. Rapaport *et al.*, Nucl. Phys. **A427**, 332 (1984).
[43] W. P. Alford *et al.*, Phys. Rev. C **48**, 2818 (1993).
[44] J. Rapaport *et al.*, Nucl. Phys. **A410**, 371 (1983).
[45] M. B. Aufderheide, Nucl. Phys. **A526**, 161 (1991).